

Primary brain cell infection by *Toxoplasma gondii* reveals the extent and dynamics of parasite differentiation and impact on neuron biology.

Thomas Mouveaux ¹, Emmanuel Roger ¹, Alioune Gueye ¹, Fanny Eysert ², Ludovic Huot ¹, Benjamin Grenier-Boley ², Jean-Charles Lambert ² and Mathieu Gissot ^{1,*}.

1. Univ. Lille, CNRS, Inserm, CHU Lille, Institut Pasteur de Lille, U1019 - UMR 9017 - CIIL - Center for Infection and Immunity of Lille, F-59000 Lille, France.
2. Univ. Lille, Inserm, Institut Pasteur de Lille, U1167, F-59000 Lille, France.

* To whom correspondence should be addressed: mathieu.gissot@pasteur-lille.fr

ABSTRACT

Toxoplasma gondii is a eukaryotic parasite that form latent cyst in the brain of immunocompetent individuals. The latent parasites infection of the immune privileged central nervous system is linked to most complications. With no drug currently available to eliminate the latent cysts in the brain of infected hosts, the consequences of neurons long-term infection are unknown. It has long been known that *T. gondii* specifically differentiate into a latent form (bradyzoite) in neurons, but how the infected neuron is responding to the infection remain to be elucidated. We have established a new *in vitro* model resulting in the production of fully mature bradyzoites cysts in brain cells. Using dual, host and parasite, RNA-seq we characterized the dynamics of differentiation of the parasite, revealing the involvement of key pathways in this process. Moreover, we identified how the infected brain cells responded to the parasite infection revealing the drastic changes that take place. We showed that neuronal specific pathways are strongly affected, with synapse signaling being particularly affected, especially glutamatergic synapse. The establishment of this new *in vitro* model allows to investigate both the dynamics of the parasite differentiation and the specific response of neurons to the long term infection by this parasite.

INTRODUCTION

Toxoplasma gondii is a unicellular eukaryotic pathogen. It belongs to the apicomplexan phylum, which encompasses some of the deadliest pathogens of medical and veterinary importance, including *Plasmodium* (the cause of malaria), *Cryptosporidium* (responsible for cryptosporidiosis) and *Eimeria* (coccidiosis). *T. gondii* is an obligate intracellular parasite. Although toxoplasmosis is generally asymptomatic, it can lead to the development of focal central nervous system (CNS) infections in immunocompromised hosts. In addition, *Toxoplasma* is also a clinically important opportunistic pathogen that can cause birth defects in the offspring of newly infected mothers. The worldwide seroprevalence of *T. gondii* infection is estimated between 30 and 70% in humans, although it differs significantly depending on the geographical areas [1].

The life cycle of *T. gondii* is complex, with multiple differentiation steps that are critical to parasite survival in human and feline hosts [2]. Infection by oocysts containing sporozoites shed by cats or by bradyzoites contaminating ingested meat leads to differentiation into the rapidly growing tachyzoites that are responsible for the clinical manifestations in humans. The conversion of the tachyzoites into bradyzoites, responsible for the acute or the chronic phase of the disease, respectively, is made possible by the unique ability of the tachyzoite to spontaneously differentiate into bradyzoite in specific cell type such as muscle cells or neurons. These latent bradyzoites are thought to persist in the infected host for prolonged period due to their ability to evade the immune system and to resist commonly used drug treatments. Bradyzoites have also the ability to reactivate into virulent tachyzoites and cause encephalitis, in particular in immunocompromised hosts [3]. Therefore, the tachyzoite to bradyzoite interconversion is a critical step for the pathogenesis and survival of the parasite. *T. gondii* tachyzoite to bradyzoite stress-induced differentiation has been extensively studied *in vitro* using alkaline stress and other stimuli [4]. However, this process does not produce persisting cyst that express mature bradyzoite markers [5]. It merely reflects the complexity of the process observed *in vivo*. For example, much higher rates of spontaneous differentiation are observed in primary neurons [6]. However, infection of primary neurons were only performed for short periods (up to 4 days) [7–10]. Therefore, a global understanding of the kinetics and dynamics of

differentiation is lacking due to widespread use of the imperfect, but easy to handle, stress induced differentiation model.

T. gondii latent infection of the immune privileged CNS is linked to most complications that can be fatal in the case of reactivation of bradyzoite cysts in immune-deficient hosts. These intracellular parasites migrate to the brain and cross the blood–brain barrier (BBB) by a Trojan horse mechanism [11] or by compromising the permeability of the BBB after infection and lysis of epithelial cells [12]. After reaching the CNS, the parasites can invade all nucleated cells, although infection is detected and persist in neurons *in vivo* [13]. Consistent with the ability of this parasite to infect and persist in neurons, *T. gondii* has been linked to behavioral changes in rodent models. The most prevalent study reported the ability of the parasite to specifically manipulate the behavior of rodents in relation to predator–prey interaction. In these studies, chronically infected mice were specifically impaired for their aversion to feline urine scent [14,15]. Moreover, *T. gondii* infection have been directly implicated in modulating dopamine production [16], decreasing levels of norepinephrine and glutamate [17,18], altering GABAergic signaling [19], thereby inducing an imbalance in neuronal activity [20], inducing neurons apoptosis [21] and altering synaptic protein composition [22]. Chronic toxoplasmosis is also correlated with the establishment of a low grade neuroinflammation characterized by the production of proinflammatory cytokine interferon-gamma (IFN-g). IFN-g is critical to control parasite replication [23] by inducing cell autonomous immunity of immune resident brain cells notably astrocytes and microglia. Recently, *T. gondii* induced neuroinflammation have also been linked to behavior changes in rodents [24,25] indicating that infection likely causes direct and indirect effects on neuronal functions. In humans, a growing number of studies have linked *T. gondii* to psychiatric diseases such as schizophrenia [26,27], behavior alterations [28] and neurodegenerative diseases such as Parkinson and Alzheimer disease [29]. Indeed, chronic neuroinflammation may also cause neurological disorders either by producing neurodegeneration, neurotransmitter abnormalities and therefore altering the neuron functionality [30]. *T. gondii* infection may therefore have lifelong effects on the CNS of immunocompetent hosts.

Although global measurement of alteration at the whole brain level [31,32] clearly indicates broad changes in neuron biological functions, what are the extent of the modifications of the individual neuron during long-term infection is not understood. Similarly, *in vivo* studies could not address the kinetics of the spontaneous differentiation of the parasite. To address this question, we reasoned that an *in vitro* culture of neurons would require the support of other cells such as astrocytes, which provide metabolic support for neurons and promote the function of synapses [33]. Therefore, we infected a complex primary brain cell culture with *T. gondii* tachyzoites to study the spontaneous differentiation dynamics and the host cell response to infection during differentiation and once the cysts are established. We show here that spontaneous differentiation occurs using this *in vitro* system and can be maintained for at least 14 days. Using RNA-seq, we characterized the dynamic changes in both parasite and host cell gene expression. We investigated the kinetic of parasite differentiation and the alteration of the brain cell gene expression after infection. We showed that this model produced infective bradyzoite cysts after 2 weeks of culture mirroring *in vivo* models. Thus, the *in vitro* model we established offers a unique opportunity to dissect the molecular mechanisms of parasite differentiation and the consequences of *T. gondii* infection on neuron biology.

MATERIAL AND METHODS

Parasite strains and culture

Toxoplasma gondii tachyzoites of the 76K was propagated *in vitro* in human foreskin fibroblasts (HFF) using Dulbeccos's modified Eagles medium supplemented with 10% fetal calf serum (FCS), 2mM glutamine, and 1% penicillin-streptomycin. The Pru $\Delta ku80$ strain contains a knock-out of the *ku80* gene increasing the likelihood of homologous recombination to occur and the transfection to succeed. Tachyzoites were grown in ventilated tissue culture flasks at 37°C and 5% CO₂. Prior to mice infection intracellular parasites were purified by sequential syringe passage with 17-gauge and 26-gauge needles and filtration through a 3- μ m polycarbonate membrane filter.

Brain cell culture

Animal housing and experimentation were carried out in accordance with the French Council in Animal Care guidelines for the care and use of animals and following the protocols approved by the Institut Pasteur de Lille ethical committee. Primary neuronal cultures were obtained from hippocampus of postnatal (P0) rats as described previously [34]. Briefly, after the dissection of the brains, hippocampi were washed three times in HBSS (HBSS, 1-M HEPES, penicillin/streptomycin, and 100-mM sodium pyruvate, Gibco) and were dissociated via trypsin digestion (2.5%, 37°C, Gibco) for 7min. Next, hippocampi were incubated with DNase (5mg/mL, Sigma) for 1min and washed again in MEM medium supplemented with 10% SVF, 1% Glutamax, 0.8% MEM vitamins, 0.5% penicillin/streptomycin, and 0.45% d-glucose (Sigma). With a pipette, hippocampi were mechanically dissociated and resuspended in Neurobasal A medium (Gibco) supplemented with 2% B27 (Gibco) and 0.25% GlutaMax. In total, 200,000 neurons were seeded per well in 24-well plates. Neurons were maintained at 37°C in a humidified 5% CO₂ incubator.

RNA sample collection and library preparation

RNA samples were collected after infecting the primary brain cell cultures by the 76K strain for 24, 48, 96 hours, 7 and 14 days. Uninfected brain cell culture samples were collected at the same time than the 24 hours infected cells time-point. Infected and uninfected cells were scrapped from the plates and lysed in Trizol. RNA was extracted as per manufacturer instruction and genomic DNA was removed using the RNase-free DNase I Amplification Grade Kit (Sigma). All RNA samples were assessed for quality using an Agilent 2100 Bioanalyzer. RNA samples with an integrity score greater than or equal to 8 were included in the RNA library preparation. Triplicate (biological replicate) were produced for each conditions. The TruSeq Stranded mRNA Sample Preparation kit (Illumina) was used to prepare the RNA libraries according to the manufacturer's protocol. Library validation was carried out by using DNA high-sensitivity chips passed on an Agilent 2100 Bioanalyzer. Library quantification was carried out by quantitative PCR (12K QuantStudio).

RNA-seq and analysis

Clusters were generated on a flow cell with within a cBot using the Cluster Generation Kit (Illumina). Libraries were sequenced as 50 bp-reads on a HiSeq 2500 using the sequence by synthesis technique (Illumina). HiSeq control software and real-time analysis component were used for image analysis. Illumina's conversion software (bcl2fastq 2.17) was used for demultiplexing. Datasets were aligned with HiSAT2 v2.1.0 [35] against the *T. gondii* ME49 genome from (ToxoDB-39) [36] and to the rat genome (*Rattus norvegicus* Rn6 (UCSC)). Expression for annotated genes was quantified using htseq-count and differential expression measured by DESeq2. P-values for multiple testing were adjusted using the Benjamini-Hochberg method. Differentially expressed genes with adjusted p-value below 0.05 and log2 fold-change above 2 were considered in this study. Gene ontology was performed using the PANTHER [37] (Version 15) Overrepresentation Test (Released 20190711) surveying GO Slim Biological pathways using the Fisher statistical test for significance. RNA-seq data that support the findings of this study have been deposited in the GEO database under the accession number GSE168465.

Immunofluorescence analysis

Infected and uninfected brain cells cultures were fixated using 4% PFA for 30 minutes. The coverslips were incubated with primary antibodies and then secondary antibodies coupled to Alexa Fluor-488 or to Alexa-Fluor-594. Primary antibodies used for IFAs include: anti-TgEno2, anti-TgSAG1, anti-MAP2 and anti-GFAP and were used at the following dilution 1:1000, 1:1000, 1:500 and 1:500 respectively. A lectin from *Dolichos biflorus* coupled to fluorescein was also used at 1:400 dilution to identify the parasitic vacuoles. Confocal imaging was performed with a ZEISS LSM880 Confocal Microscope. All images were processed using Carl Zeiss ZEN software. Quantification of immunofluorescence assays was carried out manually by counting the concerned signal corresponding to the organelle by visual observation. Signal corresponding to 100 parasites was counted for each replicate.

Western-Blot

Total protein extracts representing infected or uninfected cells were resuspended in 1X SDS buffer. The protein samples were then fractionated on a 10% SDS-polyacrylamide electrophoresis gel and

then transferred onto a nitrocellulose membrane. The anti-VGLUT1 (cat # 48-2400, Thermo-Fischer) and anti GAPDH antibodies were used at a 1:1000 dilution. Chemiluminescent detection of bands was carried out by using Super Signal West Femto Maximum Sensitivity Substrate.

RESULTS

Establishment of the in vitro infection model of primary brain cell culture

To produce the primary brain cell culture, we extracted brain cells from newborn rats and placed them in culture for 14 days prior to infection. By immunofluorescence, we quantified that neurons represented at least 30 % of the cells present in culture as identified by the MAP2 marker (Figure S1A). Astrocytes, as identified by the GFAP marker, represent more than 50 % of the total cells while glial cells and oligodendrocytes represented around 20 % of all the cells (Figure S1A). This percentage did not vary over time (Figure S1A) or after infection (Figure S1B). Infection occurred and persisted in neurons and astrocytes and was maintained over time with a similar percentage of cells being infected until the 14 days time point (Figure 1A). To characterize the *T. gondii* spontaneous differentiation dynamic in this *in vitro* model, we followed the expression of tachyzoite (TgSAG1) and bradyzoite (Cyst wall labelled by *Dolichos biflorus* lectin and p21, a late bradyzoite marker [38]) markers over time. Spontaneous differentiation occurred within a short time frame in the brain cells with the appearance of parasites expressing a marker of the cyst wall (labelled by the *Dolichos biflorus* lectin) 24h after infection representing more than 90 % of the parasite population after 96h (Figure 1B). Parasites expressing the tachyzoite marker TgSAG1 followed a reverse trend (Figure 1C). We noted the appearance of the late bradyzoite marker (p21) in cysts 96h after infection and more than 70 % of the cyst population was positive for this marker after 7 days (Figure 1D). Interestingly, we observed transitioning parasites until 48h of infection (expressing both tachyzoite and bradyzoite markers TgSAG1 and *D. fluorus* lectin; Figure 1E), while all the parasites expressing p21 were also positive for the *D. fluorus* lectin (Figure S1C). Imaging of parasites at 7 days after infection demonstrates that the parasites converted to bradyzoite and established latency in both astrocytes and neurons (Figure 1F) in this *in vitro* model.

Dual RNA-seq on the parasite and host cell during the spontaneous parasite differentiation

To assess the transcriptome changes during the parasite spontaneous differentiation and the host response to infection, we collected triplicate RNA sample of infected primary CNS cell culture at 1d,

2d, 4d, 7d and 14d post-infection (Figure 2A). We analyzed transcriptomic profiles of both the parasite and host cells (Figure S2A and S2B). Sequencing reads were assigned to the rat or to the parasite genome (Table 1). For each time point, the infected host transcriptome was compared to a non-infected host cell culture. Reads assigned to the parasite genome were compared to a purified tachyzoites derived sequencing reads. We used a p-value cut-off of 0,05 and a minimum 2-fold change to identify differentially expressed genes (DEG) using the DESEQ2 program (Table 2). We performed a principal component analysis (PCA) to identify how each condition was clustering (Figure 2B and 2C). On the parasite side, the PCA analysis revealed that expression was similar between the time point 1d and 2d while 4d appeared to represent the transition from the tachyzoite to the bradyzoite specific expression observed at day 7d and 14d (Figure 2B). On the host side, PCA showed that the response to infection was different for the 1d and 2d time points compared to 7d and 14d (Figure 2C).

Spontaneous parasite differentiation transition is reflected by specific expression patterns

We compared the parasite expression profiles obtained for each time point of the brain cell infected culture (Figure 3A). Differential expression mirrors the timing of spontaneous differentiation. Indeed, most of the changes are initiated at 1d and 2d p.i and are maintained during later time point (Figure 3A, 636 DEG). At these time points, parasites are still transitioning (Figure 3A, Table 2 and Table S1). A turning point is observed at 4d post-infection when the late bradyzoite marker are detected in the *in vitro* culture (Figure 1), and parasite further differentiate to mature bradyzoites at day 7 and 14 (Figure 3A, 1200 DEG common to 4d, 7d and 14d). Little changes are identified in the parasite transcriptome between day 7 and day 14 (Figure 3A, Table S1). The list of common DEGs between each time points encompasses the main bradyzoite markers such as BAG1, ENO1, LDH2, and BRP1 (Table 3). In contrast, tachyzoite markers (LDH1, ENO2 and SAG1) were repressed with a different dynamic (Table 3). While SAG1 is already repressed 1d after infection, ENO2 and LDH1 were significantly repressed only after 4d of infection (Table 3). We performed pathway-enrichment analyses based on the 1200 common DEGs for the 4d, 7d and 14d time points, and found that classical pathways known to be repressed such as translation are overrepresented (Figure S3). Similarly, the GO enriched

pathways based on the upregulated genes are in line with the carbohydrate metabolism switch known to happen during differentiation (Figure S3) [39].

Parasites established in brain cell culture are mature bradyzoites

Expression profiles during stress induced differentiation were already characterized in numerous studies [40–42]. We compared the expression profiles of up and down-regulated genes after stress induced differentiation [42] with the brain cell infected culture RNA-seq results. We showed that more than 80% of the up-regulated genes (fold change >2 ; pvalue $<0,05$) after stress induced differentiation are common in these two models of in vitro produced bradyzoites (Figure S4A, 255 DEG). While most of the upregulated genes are common between the stress induced differentiation and the 1d and 2d time points of our dataset, a specific expression profile is revealed at 4d (104 DEG only in 4d and 75 shared between 4d and 7d) and 7d or 14d (78 and 85 DEG respectively and 161 shared between the two time points). Similar results are observed for down-regulated genes (Figure S4B). This may indicate that contrary to stress-induce differentiation, bradyzoites produced in brain cells may differ at later time points. These late time-point brain cell producing bradyzoites may better represent the slow maturation of bradyzoites that is observed *in vivo*. To address this question we compared our dataset to expression profiles obtained from bradyzoites purified from mouse brain [32] (Figure 3A). We noticed that more than 70 % of the DEG are identical in the mature bradyzoites and in our dataset indicating that the expression profile established in in vitro culture is close to the one established in mature bradyzoites purified from brains (Figure 3C). To investigate if the bradyzoites cysts produced *in vitro* using brain cells could resemble the mature cysts produced *in vivo*, we tested the ability of these parasite form to establish an infection in mice after oral gavage. In this experiment, the cysts have to go through the digestive system and released the bradyzoites in the gut to proceed to the infection of intestine cells. The parasites will from there turn into tachyzoites and eventually produce cysts in the brains. We used the cysts formed *in vitro* after 7 or 14 days of differentiation and uninfected brain cells to gavage mice. Six weeks after gavage, we collected the brains of the infected mice and probed for the presence of cysts. All the mice that were gavaged using 14 days *in vitro* cysts were successfully infected and presented cysts in their brain, while only one mouse presented cysts when using 7 days *in*

vitro cysts (Figure 3C) indicating that 14 days cysts may have gone through more maturation steps. No cysts were found in the mice infected by brain cells alone (Figure 3C).

Expression patterns during parasite differentiation suggest an overhaul of invasion and host-cell remodeling activities in the bradyzoite.

Tachyzoite have a distinctive ability to modulate the expression of host cells by injecting parasite proteins to hijack the host's regulatory pathways [43]. Very limited information is available about the expression of exported proteins from bradyzoites [44,45] and their abilities to manipulate the host cells. We examined the expression of known effectors proteins that are known to be exported to the host-cell cytosol and nucleus [43]. In our dataset, we found that most of the known effectors were downregulated during differentiation indicating that their expression is no longer needed for bradyzoite development (Table 4). Notably, TgIST was the only effector that presented a similar expression level in tachyzoite and in bradyzoites and this for all time points examined (Table 4). As shown before for tachyzoite and bradyzoite markers (Table 3), day 4 represented a braking point where the bradyzoite expression program replace that of the tachyzoite. Exploring the expression of other potential effectors suggested that a complete transformation in the expression of these proteins is taking place during differentiation (Table S2). We also investigated the expression of proteins specialized in the invasion of host-cells to verify if the bradyzoites also adapted their invasion machinery. Surprisingly, most of the proteins known to be important for tachyzoite invasion were downregulated (Table 5). Instead, a specialized subset of genes (RON2L1, RON2L2, sporoAMA1, AMA2 and AMA4 to a lesser extent) were over-expressed in bradyzoite especially at later time points. These proteins could potentially functionally replace in bradyzoite the tachyzoite specific AMA1 and RON2 proteins (Table 5). In line with these profound changes, the expression pattern of ApiAP2 transcription factors that may be responsible for the establishment of the specific expression profile varied also during differentiation (Figure S5). ApiAP2 expression profiles grouped in different clusters (Figure S5A): a first bradyzoite cluster induced early during differentiation that contained AP2IX-9 [46], a second bradyzoite cluster with factors induced later during differentiation containing AP2XI-4 [47] and a tachyzoite specific cluster with AP2IX-5 [48] and AP2XI-5 [49]. Principal component

analysis based on the ApiAP2 expression profiles mirrored the transition during differentiation (Figure S5B). ApiAP2 transcription factors that may control different process during differentiation may be present in the bradyzoite cluster.

Brain cell culture showed differential response to tachyzoite and bradyzoite infection.

On the host side, infection by *T. gondii* tachyzoites triggered a strong response of the host cells (Table 2 and Table S3). This response is in part stable during the 14d of infection process since most of the DEGs are common between each time point (834 DEG, Figure 4). However, early response at 1d (with 521 unique DEG) and 2d (318 DEG only present in at day 1 and 2 p.i) represented a specific response to acute infection (Figure 4). We also noted that latter time points (7d and 14d p.i) presented a unique differential expression pattern (531 DEG specific from 14d and 433 only common to 7d and 14d). This indicates that a distinctive host response to tachyzoite infection (early time points) is induced when compared to the time where cysts are established (7 and 14 days p.i). We separated DEG between upregulated (Figure S6A) and downregulated (Figure S6B) and we identified similar trends with a number of DEG being shared between each time point and representing the common response to infection. We also noted that a subset of DEG was up-regulated or downregulated at the first time points while a specific response was also emerging for later time points.

Upregulation of immune related pathways is a hallmark of T. gondii infected brain cell culture.

We performed a pathway enrichment analysis on the rat genes that are differentially expressed when comparing the brain cell uninfected cultures to the infected cultures at different time-points (Figure 5). First, we looked into up-regulated genes that were common for all time points and identified that the main response was an immune response to the infection that lasted during the 14 days of infection (Figure 4B). In particular, the response to chemokine (GO:1990868) and the chemokine-mediated signaling pathway (GO:0070098) pathways were overrepresented (Figure 5A). Similarly, upregulated DEG belonging to the cellular response to cytokine stimulus (GO:0071345) and response to cytokine (GO:0034097) pathways were also overrepresented. Moreover, the response to interleukin-1 (GO:0070555) was also enriched in this dataset. This is in line with the neuroinflammation observed *in vivo* [50] and likely reflects the activation of astrocytes and glial cells present in the culture. This

indicates that both microglia and astrocyte present in the brain cell culture are being activated and respond strongly to the infection *in vitro*. Moreover, a specific response is observed in early time points (days 1 and 2), with a clear enrichment of genes involved in cell cycle and DNA replication arrest (GO:0045839 and GO:0051985) indicating that infection may induce an arrest of cell division of the brain cells such as glial cells present in the culture (Figure S7A). At later time points, further activation of microglia may take place with the CD80 expression along with Galactin9 expression (Figure S7B).

T. gondii infection induce a downregulation of key neuron functions and pathways.

Downregulated DEG common to all time points were analyzed using gene ontology. The synapse function was impacted at all-time points (Figure 5A). Notably, the most enriched pathways downregulated were linked to the synapse plasticity and transmission (GO:0050804, GO:0007269 and GO:0007268). In particular, the glutamatergic synapse was affected with the down-regulation of metabotropic glutamate receptors (Grm1, 2 and 4) and Glutamate ionotropic receptor (Grik1, NMDA2C and 2D) as previously described *in vivo* [18]. At later time point, the downregulation of a supplementary metabotropic glutamate receptor (Grm8) together with Homer 1 and 2 protein homologs that link the glutamate receptor to downstream signaling, indicated a potential long term impairment of the glutamate receptor signaling pathway (GO:0007215). We inspected the expression of the Grm1 protein during the infection of brain cells and confirmed the down-regulation of this protein illustrating the long-term effects of *T. gondii* infection on the glutamatergic synapse (Figure 5B and Figure S7C). Similarly, the glutamate decarboxylase isoforms (Gad1 and Gad2), responsible for GABA production in neurons, were downregulated since 1d recapitulating what was observed *in vivo* [19]. The synaptic signaling was also globally impacted with the downregulation of numerous membrane trafficking regulatory transcripts such as Synaptotagmin-1, Synapsin-2 or Otoferlin.

At early time points (1d and 2d), a specific response to infection consisted in the downregulation of axonemal dynein complex assembly (GO:0070286) pathway that suggested an arrest of axonemal assembly. At the same time point, the generation of the action potential and therefore excitability of neurons may be impacted by the downregulation of the potassium ion transmembrane transport

(GO:0071805) pathway that may occur in neurons or in astrocytes. Expression of both the regulatory membrane potential (GO:0042391) and chemical synaptic transmission (GO:0007268) pathways were also further decreased suggesting a strong impact on neuron function at late time points of infection when only bradyzoites infect neurons.

DISCUSSION

Tachyzoite to bradyzoite differentiation is a key aspect of the *T. gondii* biology and pathogenesis. To date, it has been mainly tackled through the use of an *in vitro* model of stress-induced differentiation that merely reflected the process of spontaneous differentiation observed *in vivo*. Moreover, little is known on the consequences of the long term infection of targeted host cells *in vivo* (mainly neuron and muscle cells). To better assess the spontaneous differentiation process and the host cell response to infection, we established a complex *in vitro* model where parasites are in contact with multiple cell types normally present in the brain. We reasoned that this complex environment will permit a sustainable long term infection model. We were able to produce a viable environment promoting neuron survival for a minimum time of 28 days. Using this composite *in vitro* culture system, we successfully established and maintained the infection of neurons and astrocytes by the parasite that progressively express mature bradyzoite markers for at least 14 days. Primary neuronal infection by tachyzoites and bradyzoite differentiation was already experimented in different models for short time frames (up to 4 days) [7–10]. We were able to produce cysts in neurons that could be kept in culture for at least 14 days although longer time could be achieved (30 days, data not shown). Strikingly, the cysts produced using this new *in vitro* system have all the molecular features of mature cysts previously observed *in vivo*. They are also infective by oral gavage demonstrating that the structure of the cyst wall is intact and that the *in vitro* produced bradyzoites can readily infect the mouse intestine. Surprisingly, bradyzoites were found in both neurons and astrocytes, a feature that is found in rat, mouse and human primary brain cell culture [6,9,51] but not in mouse brains where bradyzoites survival is only sustained in neurons [13]. Immune cells, that are absent in the primary brain cell culture, may be crucial to eliminate the infected astrocytes *in vivo*.

We showed that parasite expression of bradyzoite markers appeared early in the differentiation process suggesting that the parasites are switching expression patterns in the beginning of the infection process. We observed parasites that were able to co-express markers of both tachyzoite and bradyzoite forms. This illustrates that the differentiation is a dynamic process during which tachyzoites expressing bradyzoite markers can be observed until 4 days into the transition. RNA-seq also demonstrated that

tachyzoite markers expression is only significantly repressed after 4 days. Such co-expression has been also observed during differentiation *in vivo* [52]. After 7 days, the expression profiles revealed by RNA-seq suggest that the parasites present in the brain cell culture are close to what is observed for mature bradyzoites purified from infected mouse brains. We did not observe major differences in gene expression between 7 and 14 days of culture. However, only the 14 days bradyzoites containing cysts were competent for mouse infection through gavage indicating that a maturation process is still undergoing after 7 days. The parasites produced after 14 days of *in vitro* culture are therefore close to what is observed in infected brains *in vivo*.

By examining the expression pattern of transitioning parasites we observed that expression of ApiAP2 transcription factors were differentially regulated. Two clusters that appeared early and late during differentiation were identified and may coordinate the dynamic expression profiles observed in the brain cell culture. Interestingly, the over-expression of BFD1, the master switch of differentiation [42], was only observed from 4 days on, although its expression might be regulated through a post transcriptional mechanism. This indicates that multiple layers of regulation may be essential to produce mature bradyzoites.

We have also identified that the expression of the major tachyzoite effectors of host-cell manipulation were repressed during differentiation with the exception of TgIST. This suggests that the bradyzoites express a new set of proteins to enable their persistence in neurons. It would be interesting to characterize the proteins that are specifically expressed during differentiation and that have the potential to be exported in the host cell. We observed the same phenomenon for proteins known to be involved in invasion. Invasion proteins such as AMA1 and RON2, that are key to form a tight connection between the invading parasite and host cell membranes, may be replaced in the bradyzoites by AMA2 or sporoAMA1 and RON2L1 or RON2L2. This change may be necessary for the bradyzoites to invade specific host-cells, such as enterocytes, to complete the life cycle. These new findings are critical for understanding the fundamental changes that occur after differentiation. They suggest that bradyzoites remodel their parasite-host interaction machinery to adapt to a narrower host cell range (intestine enterocyte, neurons and muscle cells) compared to tachyzoites.

Neurons are strongly impacted by the *T. gondii* infection. We found that both GABA and glutamate signalings were disrupted in the brain cell culture much like what has been observed *in vivo* in *T. gondii* infected mouse brains. The glutamate signaling is disrupted from the beginning of the infection with the downregulation of both metabotropic glutamate receptors and glutamate ionotropic receptors. The later were shown to be repressed in mouse infected brains [53] and a process proposed to contribute to the establishment of psychiatric disorders such as schizophrenia. Thus, this study extends the number of receptors that may be downregulated during infection and further emphasize the impact of infection and inflammation on glutamate signaling.

We also discovered that early in infection the axonemal growth might be repressed. Development as well as maintenance of correct cilia structure is essential for the unique neuron sensory properties, suggesting that neuron may respond to infection by limiting their ability to transfer information. Repression of membrane trafficking regulatory mechanisms was also observed suggesting that the synapse function may be disrupted. This may be aggravated when the parasite established a long term infection, since both membrane potential and chemical synaptic transmission are further disturbed at later time point of the infection. Our data, expand and confirm the extent of neuronal function disruption during *T. gondii* infection.

T. gondii infection has been linked to change in behavior in rodents [14,15]. The strong disruption of glutamate and GABA signaling previously reported [19] is confirmed by our study and may provide a link between the behavior changes and the infection by *T. gondii*. Since we also observed a signature of a strong neuro-inflammation as was shown *in vivo*, it is difficult to define the contribution of the direct infection of neurons and the indirect effects of neuro-inflammation on the neuronal pathways. Recent data [24,25] indicate the importance of neuro-inflammation in *T. gondii* induced behavior changes. The *in vitro* system that we have developed could address the direct effect of infection by disrupting the expression of key mediators of neuro-inflammation (using RNAi) at different time point during infection and observing the direct effect of infection on neuron biology.

We have established that parasites spontaneously differentiate when infecting a primary brain cell culture. Differentiated parasites present the hallmarks of mature bradyzoites and persist in culture for

prolonged periods. Therefore, this *in vitro* system provides a unique opportunity to dissect the dynamic features of the parasite differentiation but also the direct effect of infection on neuron biology. It could also be of interest for the screen of novel molecules able to eliminate the parasite cyst once they are established in the neurons.

Funding

This work was supported by Centre National de la Recherche Scientifique (CNRS), Institut National de la Santé et de la Recherche Médicale (INSERM), and the CPER CTRL Longévité (to MG and JCL).

Acknowledgements

The authors wish to thank the BioImaging Center Lille for access to instruments and Dr. Marion for critically reading the manuscript.

Author contributions

TM: Data collection, Data analysis and interpretation; ER: Critical revision of the article, Drafting the manuscript; AG: Data collection; FE: Data collection; LH: Data collection; BGB: Data analysis and interpretation; JCL: Conception or design of the work, Drafting the manuscript; MG: Conception or design of the work, Drafting the manuscript, Data analysis and interpretation.

Bibliography

- 1 Montoya, J.G. and Liesenfeld, O. (2004) Toxoplasmosis. *Lancet Lond. Engl.* 363, 1965–1976
- 2 Kim, K. and Weiss, L.M. (2004) Toxoplasma gondii: the model apicomplexan. *Int J Parasitol* 34, 423–32
- 3 Munoz, M. *et al.* (2011) Immunology of Toxoplasma gondii. *Immunol. Rev.* 240, 269–285
- 4 Jeffers, V. *et al.* (2018) A latent ability to persist: differentiation in Toxoplasma gondii. *Cell. Mol. Life Sci. CMLS* 75, 2355–2373
- 5 Soete, M. *et al.* (1993) Toxoplasma gondii: kinetics of bradyzoite-tachyzoite interconversion in vitro. *Exp. Parasitol.* 76, 259–264

- 6 Halonen, S.K. *et al.* (1996) Growth and development of *Toxoplasma gondii* in human neurons and astrocytes. *J. Neuropathol. Exp. Neurol.* 55, 1150–1156
- 7 Bando, H. *et al.* (2019) *Toxoplasma* Effector GRA15-Dependent Suppression of IFN- γ -Induced Antiparasitic Response in Human Neurons. *Front. Cell. Infect. Microbiol.* 9,
- 8 Swierzy, I.J. *et al.* (2017) Divergent co-transcriptomes of different host cells infected with *Toxoplasma gondii* reveal cell type-specific host-parasite interactions. *Sci. Rep.* 7, 7229
- 9 Lüder, C.G.K. *et al.* (1999) *Toxoplasma gondii* in Primary Rat CNS Cells: Differential Contribution of Neurons, Astrocytes, and Microglial Cells for the Intracerebral Development and Stage Differentiation. *Exp. Parasitol.* 93, 23–32
- 10 Creuzet, C. *et al.* (1997) Neurons in primary culture are less efficiently infected by *Toxoplasma gondii* than glial cells. *Parasitol. Res.* 84, 25–30
- 11 Harker, K.S. *et al.* (2015) *Toxoplasma gondii* dissemination: a parasite’s journey through the infected host. *Parasite Immunol.* 37, 141–149
- 12 Konradt, C. *et al.* (2016) Endothelial cells are a replicative niche for entry of *Toxoplasma gondii* to the central nervous system. *Nat. Microbiol.* 1, 16001
- 13 Cabral, C.M. *et al.* (2016) Neurons are the Primary Target Cell for the Brain-Tropic Intracellular Parasite *Toxoplasma gondii*. *PLoS Pathog.* 12, e1005447
- 14 Vyas, A. *et al.* (2007) Behavioral changes induced by *Toxoplasma* infection of rodents are highly specific to aversion of cat odors. *Proc. Natl. Acad. Sci. U. S. A.* 104, 6442–6447
- 15 Abdulai-Saiku, S. and Vyas, A. (2017) Loss of predator aversion in female rats after *Toxoplasma gondii* infection is not dependent on ovarian steroids. *Brain. Behav. Immun.* 65, 95–98
- 16 Martin, H.L. *et al.* (2015) Effect of parasitic infection on dopamine biosynthesis in dopaminergic cells. *Neuroscience* 306, 50–62
- 17 Alsaady, I. *et al.* (2019) Downregulation of the Central Noradrenergic System by *Toxoplasma gondii* Infection. *Infect. Immun.* 87,
- 18 David, C.N. *et al.* (2016) GLT-1-Dependent Disruption of CNS Glutamate Homeostasis and Neuronal Function by the Protozoan Parasite *Toxoplasma gondii*. *PLoS Pathog.* 12, e1005643
- 19 Brooks, J.M. *et al.* (2015) *Toxoplasma gondii* Infections Alter GABAergic Synapses and Signaling in the Central Nervous System. *mBio* 6, e01428-01415
- 20 Tyebji, S. *et al.* (2019) Impaired social behaviour and molecular mediators of associated neural circuits during chronic *Toxoplasma gondii* infection in female mice. *Brain. Behav. Immun.* 80, 88–108
- 21 Wang, T. *et al.* (2019) From inflammatory reactions to neurotransmitter changes: Implications for understanding the neurobehavioral changes in mice chronically infected with *Toxoplasma gondii*. *Behav. Brain Res.* 359, 737–748
- 22 Lang, D. *et al.* (2018) Chronic *Toxoplasma* infection is associated with distinct alterations in the synaptic protein composition. *J. Neuroinflammation* 15, 216
- 23 Sarciron, M.E. and Gherardi, A. (2000) Cytokines involved in *Toxoplasmic* encephalitis. *Scand. J. Immunol.* 52, 534–543
- 24 Martynowicz, J. *et al.* (2019) Guanabenz Reverses a Key Behavioral Change Caused by Latent *Toxoplasmosis* in Mice by Reducing Neuroinflammation. *mBio* 10,
- 25 Boillat, M. *et al.* (2020) Neuroinflammation-Associated Aspecific Manipulation of Mouse Predator Fear by *Toxoplasma gondii*. *Cell Rep.* 30, 320-334.e6
- 26 Sølvssten Burgdorf, K. *et al.* (2019) Large-scale study of *Toxoplasma* and Cytomegalovirus shows an association between infection and serious psychiatric disorders. *Brain. Behav. Immun.* DOI: 10.1016/j.bbi.2019.01.026
- 27 Fond, G. *et al.* (2018) Latent *toxoplasma* infection in real-world schizophrenia: Results from the national FACE-SZ cohort. *Schizophr. Res.* 201, 373–380
- 28 Stock, A.-K. *et al.* (2017) Humans with latent *toxoplasmosis* display altered reward modulation of cognitive control. *Sci. Rep.* 7, 10170
- 29 Fabiani, S. *et al.* (2015) Neurobiological studies on the relationship between *toxoplasmosis* and neuropsychiatric diseases. *J. Neurol. Sci.* 351, 3–8

- 30 Tyebji, S. *et al.* (2019) Toxoplasmosis: A pathway to neuropsychiatric disorders. *Neurosci. Biobehav. Rev.* 96, 72–92
- 31 Pittman, K.J. *et al.* (2014) Dual transcriptional profiling of mice and *Toxoplasma gondii* during acute and chronic infection. *BMC Genomics* 15, 806
- 32 Garfoot, A.L. *et al.* (2019) Transcriptional Analysis Shows a Robust Host Response to *Toxoplasma gondii* during Early and Late Chronic Infection in Both Male and Female Mice. *Infect. Immun.* 87,
- 33 Benarroch, E.E. (2005) Neuron-Astrocyte Interactions: Partnership for Normal Function and Disease in the Central Nervous System. *Mayo Clin. Proc.* 80, 1326–1338
- 34 Kaech, S. and Banker, G. (2006) Culturing hippocampal neurons. *Nat. Protoc.* 1, 2406–2415
- 35 Kim, D. *et al.* (2019) Graph-based genome alignment and genotyping with HISAT2 and HISAT-genotype. *Nat. Biotechnol.* 37, 907–915
- 36 Gajria, B. *et al.* (2008) ToxoDB: an integrated *Toxoplasma gondii* database resource. *Nucleic Acids Res.* 36, D553-556
- 37 Thomas, P.D. *et al.* (2006) Applications for protein sequence–function evolution data: mRNA/protein expression analysis and coding SNP scoring tools. *Nucleic Acids Res.* 34, W645–W650
- 38 Tomavo, S. *et al.* (1991) Characterization of bradyzoite-specific antigens of *Toxoplasma gondii*. *Infect. Immun.* 59, 3750–3753
- 39 Garfoot, A.L. *et al.* (2019) Proteomic and transcriptomic analyses of early and late-chronic *Toxoplasma gondii* infection shows novel and stage specific transcripts. *BMC Genomics* 20, 859
- 40 Behnke, M.S. *et al.* (2008) The transcription of bradyzoite genes in *Toxoplasma gondii* is controlled by autonomous promoter elements. *Mol. Microbiol.* 68, 1502–1518
- 41 Singh, U. *et al.* (2002) Genetic analysis of tachyzoite to bradyzoite differentiation mutants in *Toxoplasma gondii* reveals a hierarchy of gene induction. *Mol. Microbiol.* 44, 721–733
- 42 Waldman, B.S. *et al.* (2020) Identification of a Master Regulator of Differentiation in *Toxoplasma*. *Cell* 180, 359-372.e16
- 43 Plattner, F. and Soldati-Favre, D. (2008) Hijacking of host cellular functions by the Apicomplexa. *Annu. Rev. Microbiol.* 62, 471–487
- 44 Krishnamurthy, S. and Saeij, J.P.J. (2018) *Toxoplasma* Does Not Secrete the GRA16 and GRA24 Effectors Beyond the Parasitophorous Vacuole Membrane of Tissue Cysts. *Front. Cell. Infect. Microbiol.* 8, 366
- 45 Mayoral, J. *et al.* (2020) In Vitro Characterization of Protein Effector Export in the Bradyzoite Stage of *Toxoplasma gondii*. *mBio* 11,
- 46 Radke, J.B. *et al.* (2013) ApiAP2 transcription factor restricts development of the *Toxoplasma* tissue cyst. *Proc. Natl. Acad. Sci. U. S. A.* 110, 6871–6876
- 47 Walker, R. *et al.* (2013) The *Toxoplasma* nuclear factor TgAP2XI-4 controls bradyzoite gene expression and cyst formation. *Mol. Microbiol.* 87, 641–655
- 48 Khelifa, A.S. *et al.* (2021) TgAP2IX-5 is a key transcriptional regulator of the asexual cell cycle division in *Toxoplasma gondii*. *Nat. Commun.* 12, 116
- 49 Lesage, K.M. *et al.* (2018) Cooperative binding of ApiAP2 transcription factors is crucial for the expression of virulence genes in *Toxoplasma gondii*. *Nucleic Acids Res.* 46, 6057–6068
- 50 Hwang, Y.S. *et al.* (2018) Characteristics of Infection Immunity Regulated by *Toxoplasma gondii* to Maintain Chronic Infection in the Brain. *Front. Immunol.* 9,
- 51 Fischer, H.G. *et al.* (1997) Host cells of *Toxoplasma gondii* encystation in infected primary culture from mouse brain. *Parasitol. Res.* 83, 637–641
- 52 Ferguson, D.J.P. (2004) Use of molecular and ultrastructural markers to evaluate stage conversion of *Toxoplasma gondii* in both the intermediate and definitive host. *Int. J. Parasitol.* 34, 347–360
- 53 Torres, L. *et al.* (2018) *Toxoplasma gondii* alters NMDAR signaling and induces signs of Alzheimer’s disease in wild-type, C57BL/6 mice. *J. Neuroinflammation* 15, 57

Figures

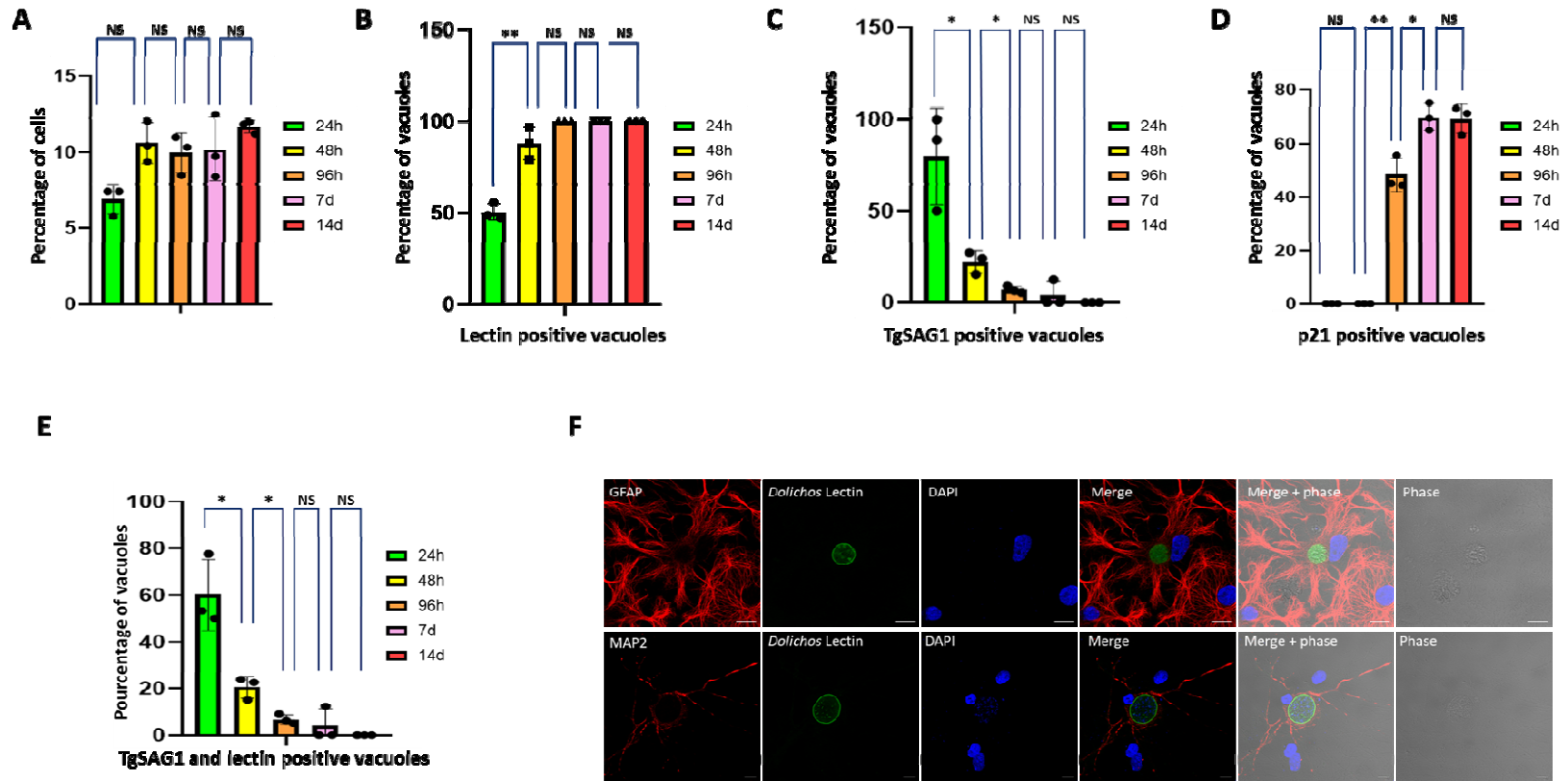


FIGURE 1

Figure 1: Critical aspects of the primary brain cell culture and its infection by *T. gondii*.

Figure 1A: Graphical representation of the number of infected cells in the brain primary cell culture. Bar graph representing the percentage of infected cells over time after 24h (green), 48h (yellow), 96h (orange), 7 days (pink) and 14 days (red) of infection. A Student's t-test was performed; two-tailed p-value; NS: $p > 0,05$; mean \pm s.d. (n=3 independent experiments).

Figure 1B: Graphical representation of the number of *D. bifluorus* lectin positive vacuoles. Bar graph representing the percentage of infected cells over time after 24h (green), 48h (yellow), 96h (orange), 7 days (pink) and 14 days (red) of infection. A Student's t-test was performed; two-tailed p-value; **: $p < 0,01$; NS: $p > 0,05$; mean \pm s.d. (n=3 independent experiments).

Figure 1C: Graphical representation of the number of vacuoles expressing the tachyzoite marker TgSAG1. Bar graph representing the percentage of TgSAG1 positive parasite vacuoles over time after 24h (green), 48h (yellow), 96h (orange), 7 days (pink) and 14 days (red) of infection. A Student's t-test was performed; two-tailed p-value; *: $p < 0,05$; NS: $p > 0,05$; mean \pm s.d. (n=3 independent experiments).

Figure 1D: Graphical representation of the number of vacuoles expressing the late bradyzoite marker p21. Bar graph representing the percentage of p21 positive parasite vacuoles over time after 24h (green), 48h (yellow), 96h (orange), 7 days (pink) and 14 days (red) of infection. A Student's t-test was performed; two-tailed p-value; *: $p < 0,05$; **: $p < 0,01$; NS: $p > 0,05$; mean \pm s.d. (n=3 independent experiments).

Figure 1E: Graphical representation of the number of vacuoles expressing the both the tachyzoite marker TgSAG1 and presenting a lectin labelling. Bar graph representing the percentage of parasite vacuole double positive for TgSAG1 and *D. bifluorus* lectin labelling over time after 24h (green), 48h (yellow), 96h (orange), 7 days (pink) and 14 days (red) of infection. A Student's t-test was performed; two-tailed p-value; *: $p < 0,05$; NS: $p > 0,05$; mean \pm s.d. (n=3 independent experiments).

Figure 1F: Immunofluorescence labelling of bradyzoites cysts in astrocytes and neurons 7 days post-infection. Confocal imaging demonstrating the presence of bradyzoites cysts (green, labelled with the *D. bifluorus* lectin) in astrocytes (upper panel, red, labelled with GFAP) or neurons (lower panel, red, labelled with MAP2). Anti-GFAP and anti-MAP2 were used as astrocyte and neuron markers, respectively. The scale bar (10 μ m) is indicated on the lower right side of each confocal image.

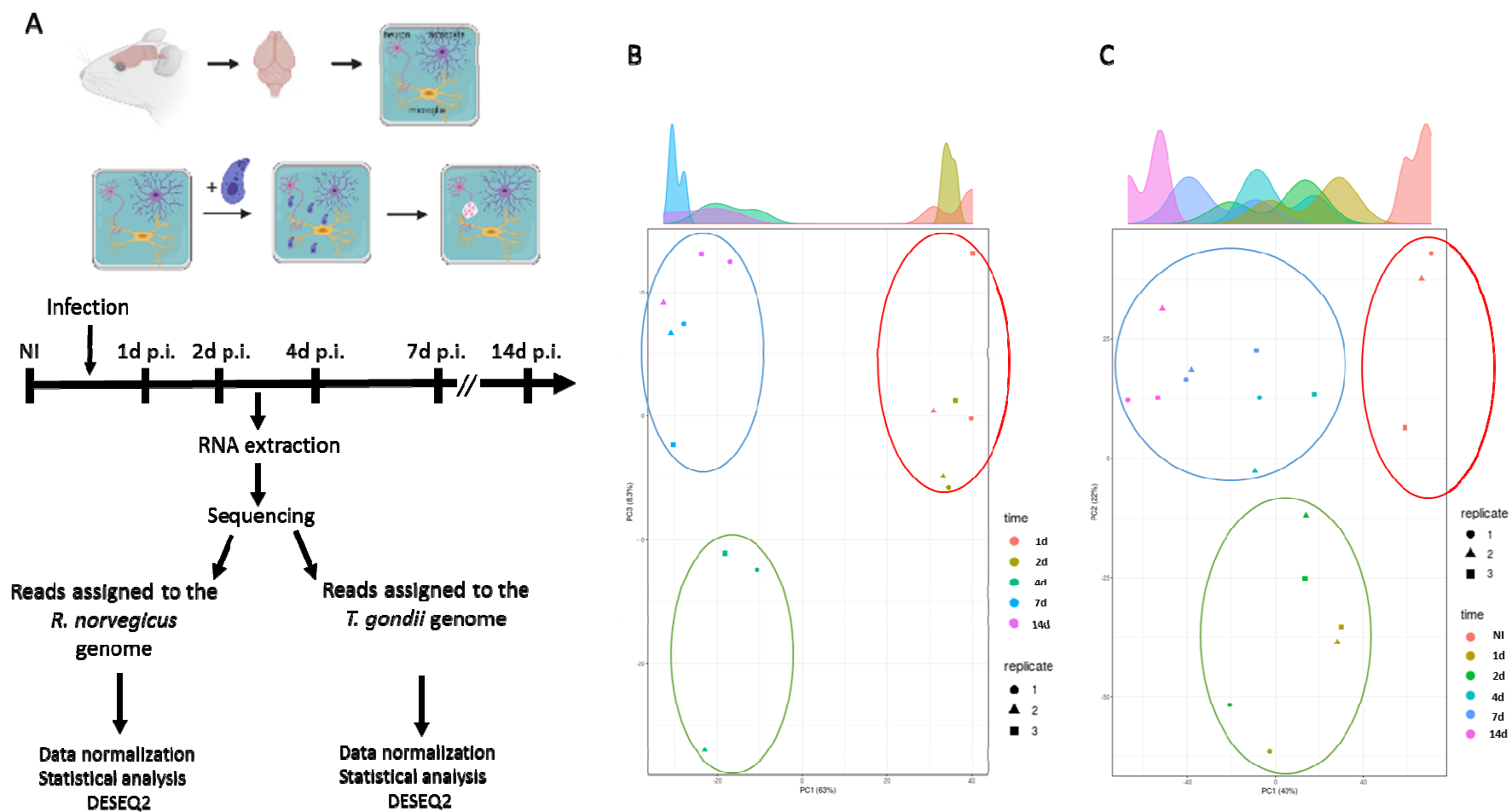


FIGURE 2

Figure 2: Dual RNA-seq on the uninfected and *T. gondii* infected primary brain cell culture.

Figure 2A: A schematics of the experiment representing the main steps of the primary brain cell culture and the time points when RNA was extracted. Libraries were created and processed to high throughput sequencing. Reads were assigned to either the *R. norvegicus* or *T. gondii* genome and DEG were assigned using DESEQ2.

Figure 2B: Principal component analysis of the *T. gondii* triplicate results for each time point. Each replicate is represented by a square, a triangle and a triangle. Each time point was assigned a color: orange (1d), green (2d), brown (4d), dark blue (7d) and pink (14d). Based on this analysis, three main grouping were found and represented by a circle: red circle (1d and 2d), green circle (4d) and blue circle (7d and 14d) suggesting sharp transition during differentiation.

Figure 2C: Principal component analysis of the *R. norvegicus* triplicate results for each time point. Each replicate is represented by a square, a triangle and a triangle. Each time point was assigned a color: orange (non-infected, NI), green (1d), brown (2d), light blue (4d), dark blue (7d) and pink (14d). Based on this analysis, three main grouping were found and represented by a circle: red circle (non-infected, NI), green circle (1d and 2d) and blue circle (4d, 7d and 14d).

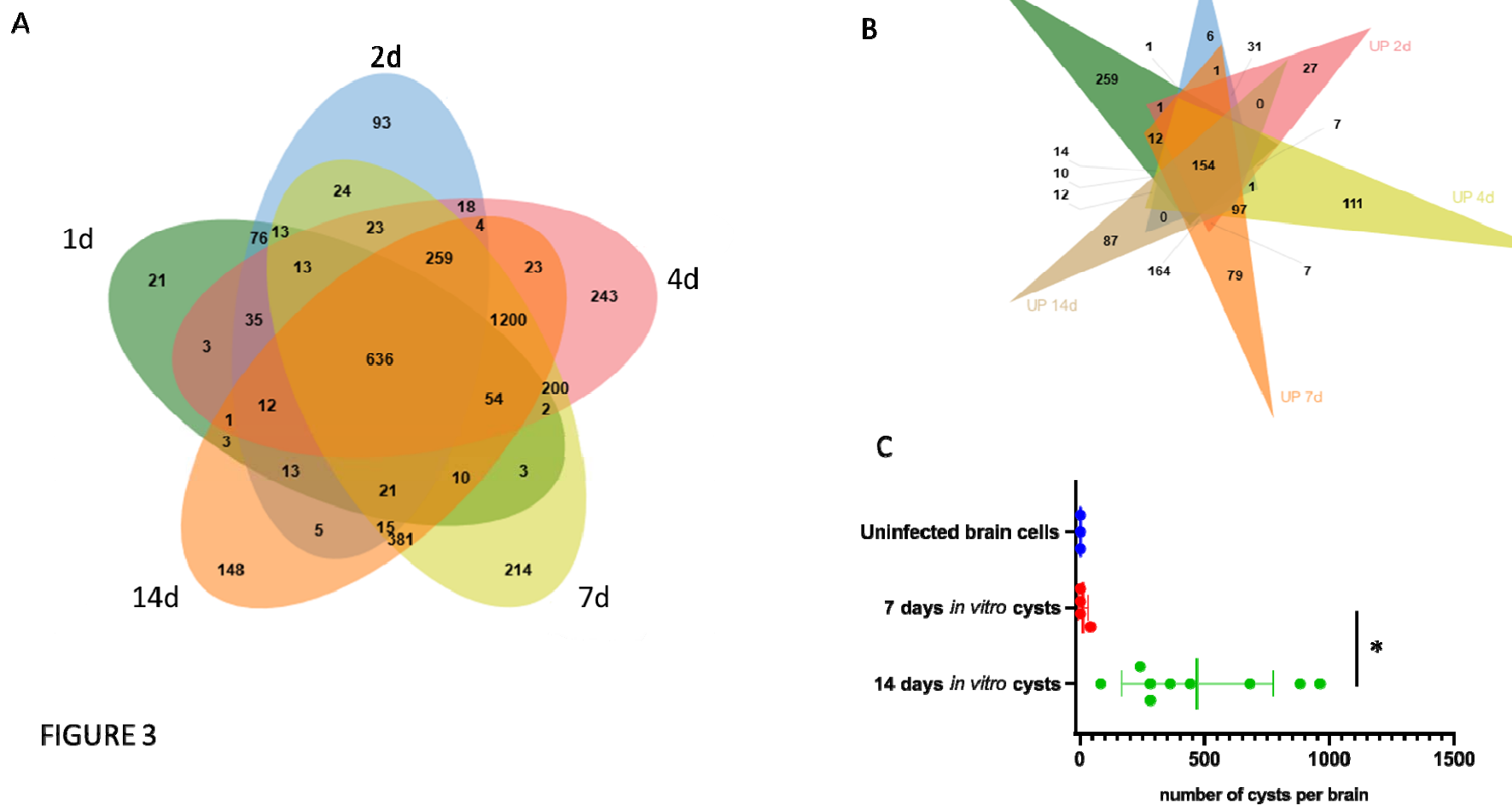


Figure 3: Bradyzoites produced in the infected primary brain cell culture are comparable to mature bradyzoites.

Figure 3A: Venn diagram of the identified DEG when comparing tachyzoites to parasite expressed genes at each time point of the brain cell culture. DEG for the 1d time point are grouped in a green circle. DEG for the 2d time point are grouped in a blue circle. DEG for the 4d time point are grouped in a red circle. DEG for the 7d time point are grouped in a yellow circle. DEG for the 14d time point are grouped in an orange circle. Number of unique or shared DEG are indicated. The total number of DEG for each time point is indicated at the bottom of the figure.

Figure 3B: Venn diagram of the identified upregulated DEG for each time point and the stress induced upregulated DEG described in the Garfoot *et al.* study [39]. DEG for the Garfoot *et al.* study are grouped in a green circle. DEG for the 1d time point are grouped in a blue circle. DEG for the 2d time point are grouped in a red circle. DEG for the 4d time point are grouped in a yellow circle. DEG for the 7d time point are grouped in an orange circle. DEG for the 14d time point are grouped in a brown circle. Number of unique or shared DEG are indicated.

Figure 3C: Bradyzoites cysts produced in vitro using the primary brain cell culture are able to transmit the infection after an oral gavage. Mice were gavaged by uninfected (blue), 7 days (red) and 14 days (green) infected brain cells. After 6 weeks, mouse brains were collected and the number of cysts per brain was measured. A Student's t-test was performed; two-tailed p-value; *: $p < 0,05$; **: $p < 0,01$; NS: $p > 0,05$; mean \pm s.d.

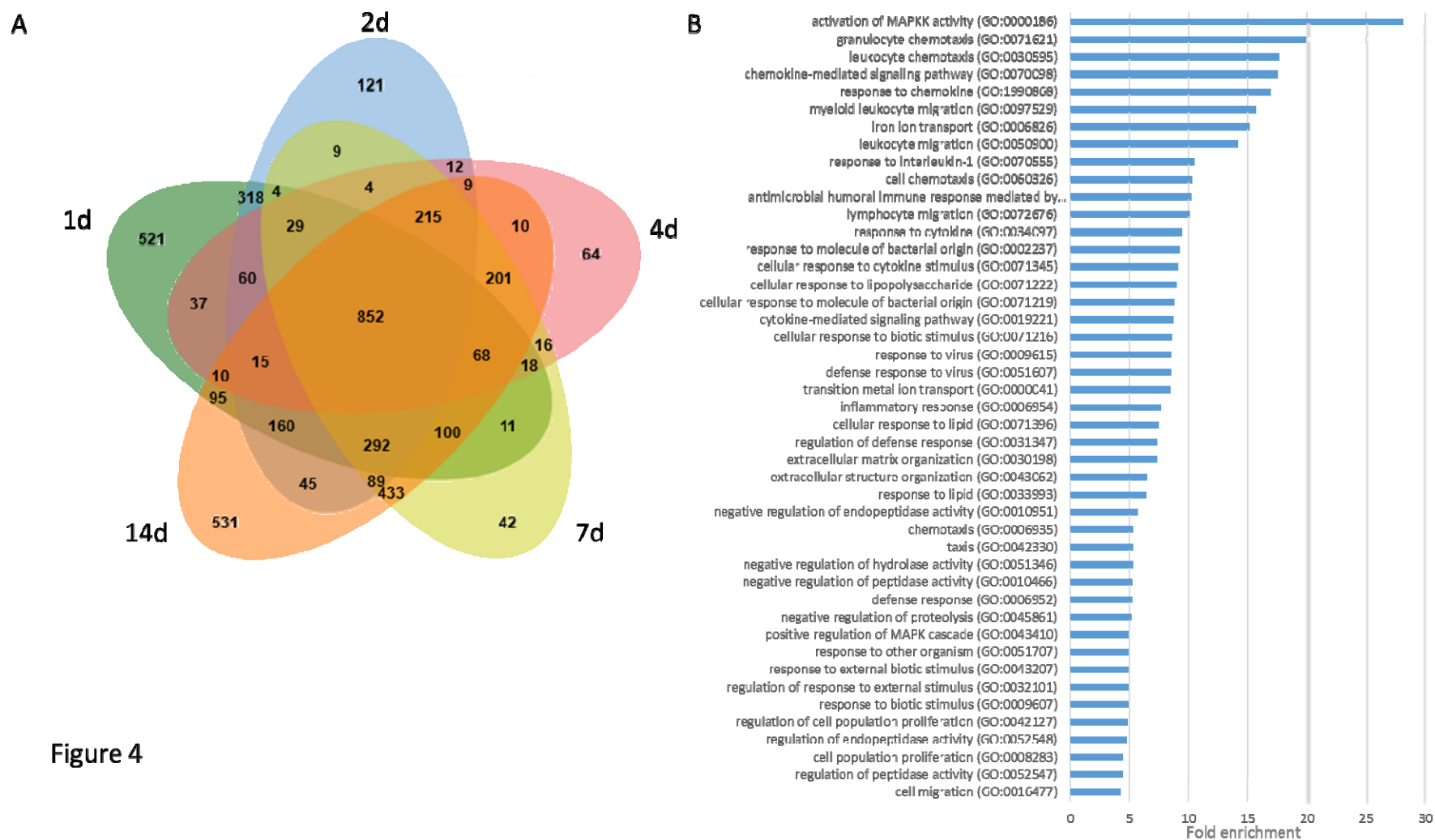


Figure 4

Figure 4: Analysis of identified *R.norvegicus* DEG in the infected primary brain cell culture when compare to uninfected samples.

Figure 4A: Venn diagram of the identified DEG for each time point. DEG for the 1d time point are grouped in a green circle. DEG for the 2d time point are grouped in a blue circle. DEG for the 4d time point are grouped in a red circle. DEG for the 7d time point are grouped in a yellow circle. DEG for the 14d time point are grouped in an orange circle. Number of unique or shared DEG are indicated. The total number of DEG for each time point is indicated at the bottom of the figure.

Figure 4B: Enriched GO pathways for upregulated DEG that are shared for all time-points infected brain cells. Pathways were selected with a FDR of 0,05 and a minimum enrichment of 4. The name of each GO pathway is indicated on the left part of the figure. Bars represent the enrichment fold.

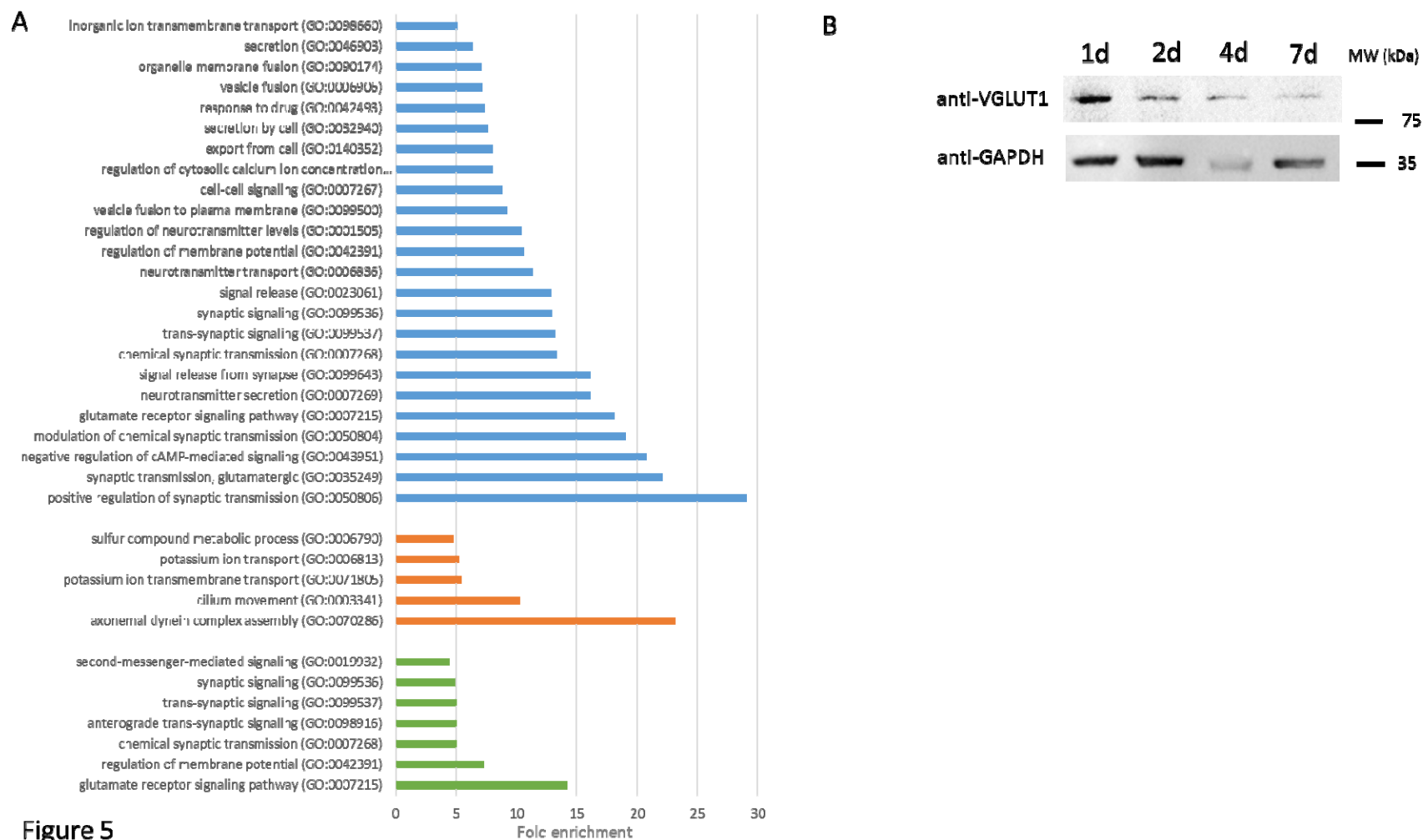


Figure 5
Figure 5: Gene ontology analysis of enriched pathways in the *R. norvegicus* samples.

Figure 5A: Enriched GO pathways for downregulated DEG that are shared for all time-points infected brain cells (blue bars), shared for 1d and 2d time points (orange bars) and shared for 7d and 14d time points (green bars). Pathways were selected with a FDR of 0,05 and a minimum enrichment of 4. The name of each GO pathway is indicated on the left part of the figure. Bars represent the enrichment fold.

Figure 5B: Western-blot showing the expression of Grm1 (VGLUT1) in neurons after 1, 2, 4 and 7 days after infection. GAPDH is used as a loading control.

Time point (days)	infection	Number of reads assigned to the rat genes	% Rat	Number of reads assigned to the <i>T.gondii</i> genes	% <i>T. gondii</i>	Number total of reads
1	infected	25252078	90.73	2579227	9.27	27831305
1	infected	22971803	94.27	1397078	5.73	24368881
1	infected	25176593	96.21	990451	3.79	26167044
2	infected	17660544	64.35	9783780	35.65	27444324
2	infected	19808387	79.82	5007576	20.18	24815963
2	infected	20621012	80.37	5036121	19.63	25657133
4	infected	18187041	64.73	10456789	35.27	28643830
4	infected	17572568	74.21	6106382	25.79	23678950
4	infected	22141916	80.89	5232408	19.11	27374324
7	infected	17699964	64.02	9949129	35.98	27649093
7	infected	16120663	68.96	7257703	31.04	23378366
7	infected	21899771	85.98	3569992	14.02	25469763
14	infected	23960501	84.48	4401325	15.52	28361826
14	infected	23324543	90.36	2488854	9.64	25813397
14	infected	23134477	91.05	2273878	8.95	25408355
	non infected	924580	99.99	3214	0.01	927794
	non infected	337050	99.99	3148	0.01	340198
	non infected	160965	99.99	1398	0.01	162363
	tachyzoites	1452	0,01	8825308	99.99	8826760
	tachyzoites	1215	0,01	8085704	99.99	8086919
	tachyzoites	966	0,01	8687601	99.99	8688567

Table 1: Number of reads assigned to the *R. Norvegicus* or *T. gondii* genes.

Comparison	Identified genes	DESeq2 DEG	Up	Down	Total cut-off >2
<i>R. norvegicus</i>					
1d vs NI	12 936	4642	1066	1523	2589
2d vs NI	12 978	3362	1050	1184	2234
4d vs NI	12 960	3114	837	784	1621
7d vs NI	12 985	3995	1150	1232	2382
14d vs NI	13 055	4907	1434	1690	3124
<i>T. gondii</i>					
1d vs Tachyzoites	7 212	2203	610	305	915
2d vs Tachyzoites	7 381	3241	842	416	1258
4d vs Tachyzoites	7 745	4634	1220	1005	2225
7d vs Tachyzoites	7 768	5002	1843	1224	3067
14d vs Tachyzoites	7 697	4459	1749	1035	2784

Table 2: Number of identified DEG for *R. norvegicus* and *T. gondii*.

Gene ID	Annotation	1d	2d	4d	7d	14d
TGME49_268860	ENO1	5,48	7,34	10,00	10,50	10,17
TGME49_291040	LDH2	7,49	8,71	9,87	10,55	10,26
TGME49_259020	BAG1	6,65	8,76	9,64	10,29	10,28
TGME49_314250	BRP1	3,71	4,84	3,47	4,05	4,33
TGME49_233460	SAG1	-1,91	-2,37	-4,65	-7,29	-6,48
TGME49_268850	ENO2	-0,46	-0,39	-1,72	-3,53	-3,15
TGME49_232350	LDH1	-0,53	-0,65	-1,54	-2,04	-1,78

Table 3: Gene expression for tachyzoite and bradyzoite markers. Log₂ fold change (FC) comparing the expression *T. gondii* transcripts at each time point of the infected brain cell culture to that of purified tachyzoites. Color gradient depends on the value of FC. Downregulated values are represented shades of green. Upregulated values are represented in shade of red. For each transcript the gene identification number (gene ID) and the corresponding annotation is also presented.

Gene ID	Annotation	1d	2d	4d	7d	14d
TGME49_308090	ROP5	-2,53	-2,67	-4,48	-3,37	-3,25
TGME49_205250	ROP18	-0,97	-0,97	-2,85	-2,28	-2,31
TGME49_258580	ROP17	-0,85	-0,66	-2,66	-2,47	-2,00
TGME49_262730	ROP16	-0,34	-0,47	-3,28	-3,66	-3,58
TGME49_275470	GRA15	-0,81	-0,75	-4,71	-5,33	-4,00
TGME49_208830	GRA16	-2,00	-1,61	-4,00	-4,75	-4,52
TGME49_230180	GRA24	-1,26	-2,11	-2,01	-3,30	-3,26
TGME49_240060	TgIST	0,46	0,49	0,59	0,71	0,54

Table 4: Gene expression for known tachyzoite effectors. Log₂ fold change (FC) comparing the expression *T. gondii* transcripts at each time point of the infected brain cell culture to that of purified tachyzoites. Color gradient depends on the value of FC. Downregulated values are represented shades of green. For each transcript the gene identification number (gene ID) and the corresponding annotation is also presented.

Gene ID	Annotation	1d	2d	4d	7d	14d
TGME49_255260	AMA1	-1,20	-1,45	-1,47	-1,25	-1,38
TGME49_294330	AMA4	-1,35	-0,58	0,31	0,05	0,52
TGME49_300130	AMA2	0,89	0,90	4,29	4,56	4,41
TGME49_315730	sporoAMA1	--	--	8,60	9,51	9,37
TGME49_265120	sporoRON2 - RON2L2	3,52	4,00	6,40	6,38	6,67
TGME49_294400	RON2L1	0,82	1,35	0,80	0,90	0,97
TGME49_310010	RON1	-0,51	-0,44	-1,59	-0,97	-0,92
TGME49_300100	RON2	-0,88	-0,83	-2,59	-2,29	-1,84
TGME49_223920	RON3	-0,53	-0,44	-2,26	-2,52	-2,08
TGME49_229010	RON4	-0,77	-0,88	-2,48	-2,27	-1,62
TGME49_311470	RON5	-1,04	-1,11	-2,29	-1,85	-1,47
TGME49_297960	RON6	-0,86	-0,87	-2,27	-1,92	-1,74
TGME49_306060	RON8	-0,69	-0,74	-2,27	-2,35	-1,90
TGME49_308810	RON9	-0,39	-0,33	-0,82	-0,80	-0,60
TGME49_261750	RON10	-0,98	-0,99	-1,09	0,00	-0,07

Table 5: Gene expression for transcripts encoding proteins known to be involved in invasion. Log₂ fold change (FC) comparing the expression *T. gondii* transcripts at each time point of the infected brain cell culture to that of purified tachyzoites. Color gradient depends on the value of FC. Downregulated values are represented shades of green. Upregulated values are represented in shade of red. Transcripts that were not detected are indicated by a double dash (--). For each transcript the gene identification number (gene ID) and the corresponding annotation is also presented.